QSAR, MOLECULAR DOCKING, MOLECULAR DYNAMICS SIMULATION, AND ADME STUDIES OF FERULIC ACID DERIVATIVES AS ANTIBACTERIAL AGENTS

Suchitra Yadav[1], Anuradha Sharma[2], Deepak Sharma[3], Mukul Arora[4], Deepanjali Baisoya[5], Mahesh Kumar[6], Balasubramanian Narasimhan[7]*

Abstract

Antimicrobial resistance is often regarded as a severe threat to human health and a significant public health concern, with numerous and complicated factors leading to its incidence and spread. The ferulic acid derivatives were selected from the reported work by Khatkar *et al*., (2015). 2D QSAR identified the nonlinear dependence of biological activity with Log P. In 2D QSAR studies, molecular descriptors include topological parameters like valence third-order molecular connectivity index ($^3\chi^V$), valence first-order molecular connectivity index ($^1\chi^V$), Kier's third-order alpha shape index ($k\alpha^3$) and Balaban, lipophilic parameter like log P, electronic parameters like Vamp Lumo and total dipole, govern the antibacterial activity of ferulic acid derivatives. The molecular docking technique predicts binding affinity, drug-receptor interaction, and orientation of drug molecules to the target site, and ADME predicts drug likeliness. Molecular docking studies signify that unds **18, 15, 21, 32,** and **30** score best against protein transcriptional regulation (PDB ID: 5X14). Based on QSAR, molecular docking, molecular dynamics simulation, and ADME studies were employed and show an excellent ADME profile by the Lipinski rule of five. The study suggests that compounds **18, 15, 21, 32,** and **30** could be lead structures for advanced research in antimicrobial resistance.

Keywords: Ferulic acid, Antimicrobial activity, QSAR, Molecular Docking, Molecular Dynamics Simulation, ADME & Transcriptional Regulation

[1,2]Faculty of Pharmaceutical Sciences, Deen Dayal Rustagi College of Pharmacy, Gurgaon, Haryana, India – 122504.
[3,4,5]Faculty of Pharmaceutical Sciences, B.S. Anangpuria Institute of Pharmacy, Faridabad, Haryana, India – 121004.
[6,7]Faculty of Pharmaceutical Sciences, Maharshi Dayanand University, Rohtak, Haryana, India – 124001

***Corresponding Author:**
Prof. Balasubramanian Narasimhan
*Faculty of Pharmaceutical Sciences, Maharshi Dayanand University, Rohtak, Haryana, India – 124001
Email: naru2000us@yahoo.com

DOI: 10.48047/ecb/2023.12.si5a.0372

INTRODUCTION

The number of invasive, opportunistic microbial species infections has increased dramatically in recent decades, as has the prevalence of systemic sickness [1]. The increased proportion of illnesses and inappropriate use of antimicrobials leads to antimicrobial resistance (AMR), which has become a global challenge [2,3,4]. If antimicrobial resistance (AMR) is not managed, the number of fatalities related to it could rise deaths from 700,000 to 10 million by 2050 [5].

Ferulic acid (4-hydroxy-3-methoxy cinnamic acid) is a phenolic acid derivative that was first discovered in the mid-nineteenth century from ***Ferula foetida*** (Apiaceae family) [6]. It is generally found in green vegetables, cereal bran, fruits, beer, coffee, wheat, barley, and several other species of plants [7]. The medicinal potential of Ferulic acid and its derivatives includes antioxidant [8], anticancer [9], antifungal and antibacterial [10], anti-inflammatory [11], antiviral [12], antidiabetic [13], cardioprotective [14], neuroprotective [15] activities.

Transcriptional regulators regulate the cell process, including converting DNA to RNA. Cell organism responds to a no. of intra and extracellular signals via transcriptional regulators [16]. Transcriptional factors are protein that binds to DNA sequences to regulate the expression of a given gene. Approximately 141400 transcriptional factors exist in the human genome, constituting coding genes [17].

Computer-Aided Drug Design is an emerging way of finding and designing novel beneficial therapeutic agents with the aid of computers in the drug discovery process [18]. Computational techniques play a significant role in drug development, as they lower the cost and time required to create and invent novel medications to treat diseases [19].

The QSAR correlates biological activity data with structural and physiochemical parameters of a series of molecules to find and evaluate novel compounds for favourable characteristics [20, 21]. A molecular graph in 2D-QSAR contains topological or two-dimensional (2D) data that elaborates how atoms in a molecule are bonded and how specific atoms interact (e.g., molecular connectivity indices, total path count, etc.) [22]. The goal of the QSAR model is a rational approach used to evaluate biological activity and physicochemical attributes [23].

The computational method of molecular docking is applied to measure the strength of binding between active site residues and specific compounds. Molecular docking is a useful approach for determining the compatibility of ligands with their target (receptor) and, as a result, selecting active compounds predicting their mechanism of action, and optimising the lead structure [24]. The main goals of the docking investigation are exact structural modelling and accurate activity prediction. The molecular docking technique studies the binding affinity, drug-receptor interaction, and orientation of drug molecules to the target site [25].

The Lipinski rule defines molecular features that influence a drug's absorption, distribution, metabolism, and excretion in the human body, also known as pharmacokinetics. ADME modelling has gained much interest from pharmaceutical researchers for drug discovery due to its low cost and high output [26].

In response to the initial findings, and as part of our ongoing work using Hansch analysis on the association of biological activities with different molecular structures, we provide here the QSAR, molecular docking, molecular dynamics simulation and ADME investigations of ferulic acid derivatives were synthesised by Khatkar *et al*., (2015) [27].

MATERIAL AND METHODS

2D QSAR Study

The ferulic acid derivatives (1-38) **Table 1**, selected from the reported work by Khatkar *et al.*, (2015), were sketched using **Chem Draw 19.0.** The biological activity was shown in **MIC (µM/ml).** It was changed to pMIC values to eliminate significant clumping, making it more dependable for the QSAR study, as shown in **Table 2**.

Table 1 Chemical structures of ferulic acid derivatives used in QSAR studies.

C. No.	Chemical Structure	C. No.	Chemical Structure
1	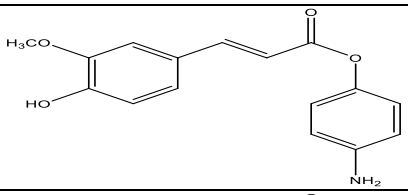	**2**	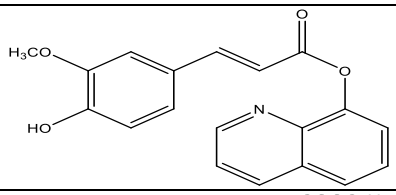
3	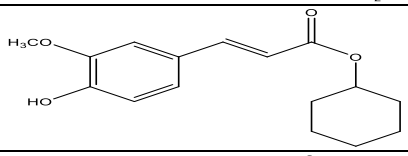	**4**	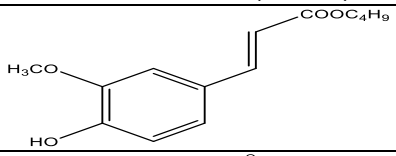
5	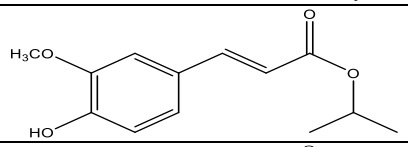	**6**	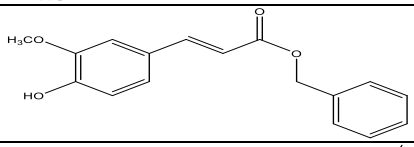
7	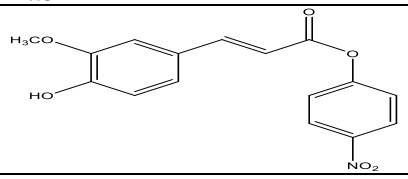	**8**	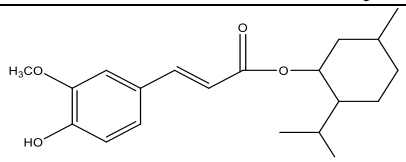
9	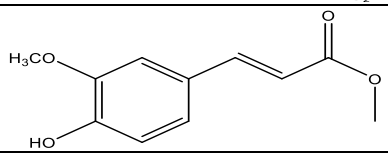	**10**	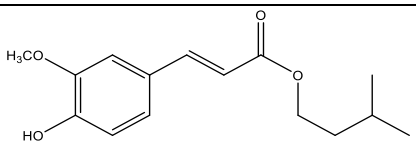
11	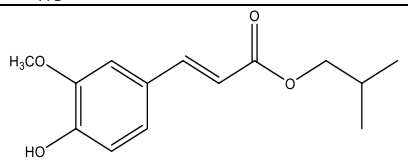	**12**	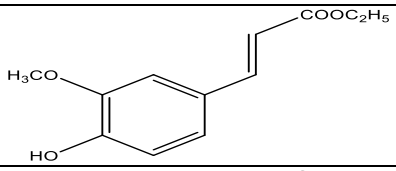
13	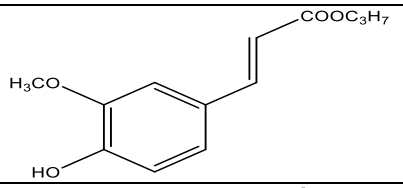	**14**	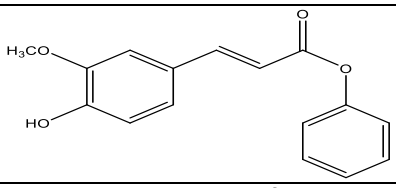
15	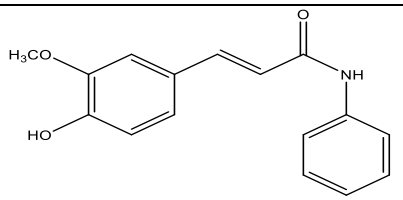	**16**	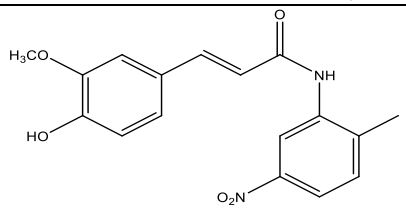
17	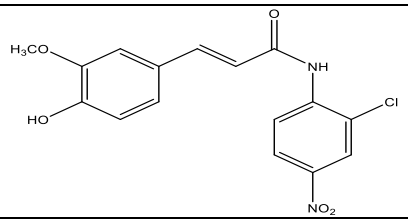	**18**	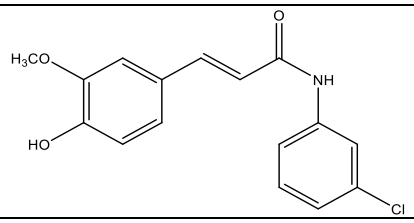
19	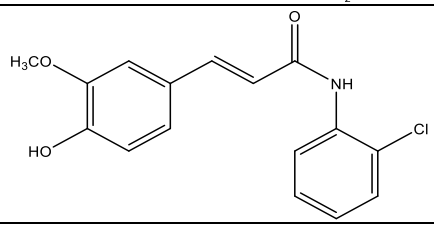	**20**	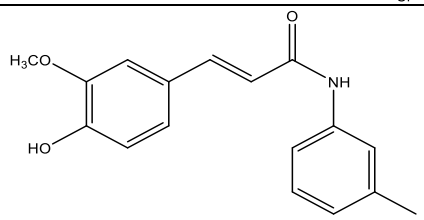

21	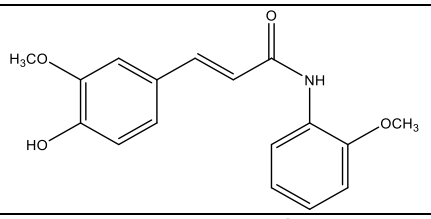	**22**	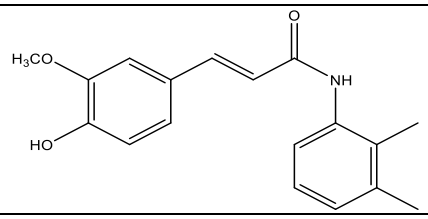
23	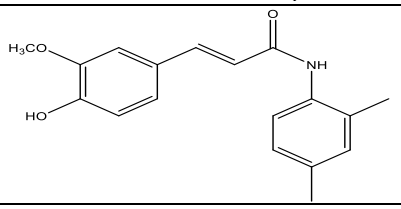	**24**	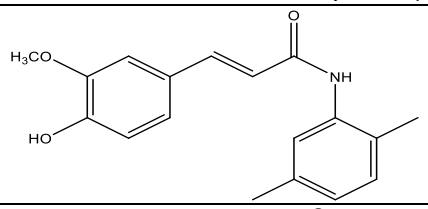
25	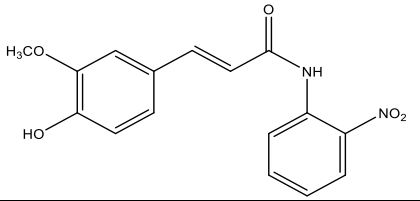	**26**	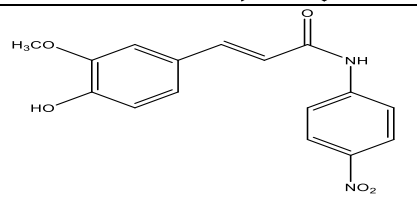
27	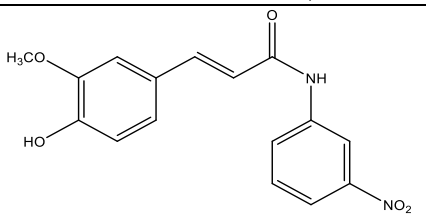	**28**	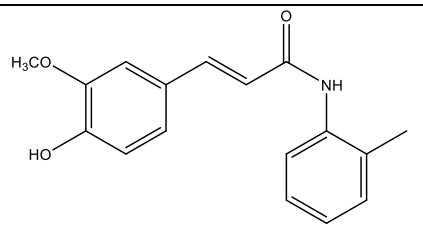
29	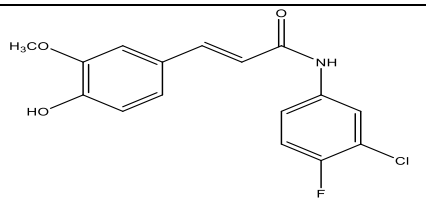	**30**	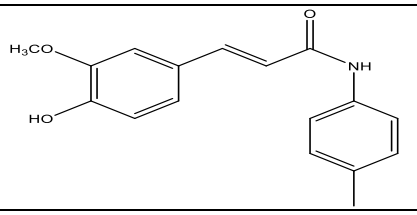
31	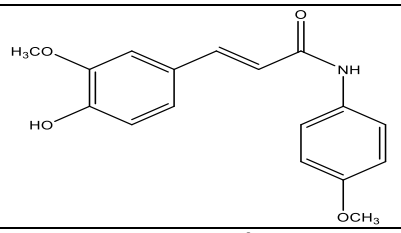	**32**	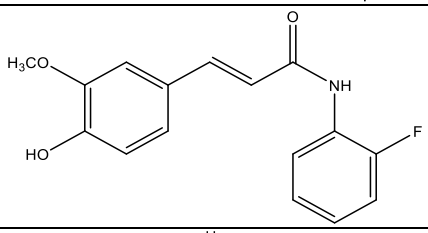
33	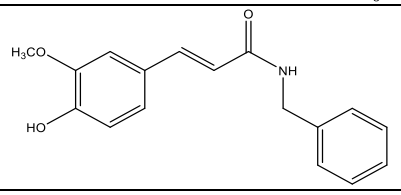	**34**	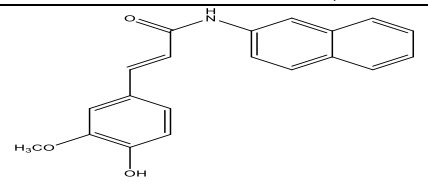
35	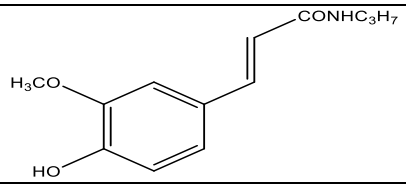	**36**	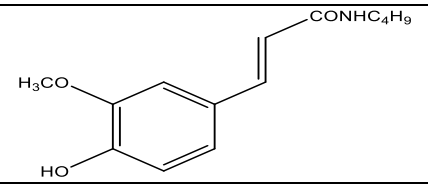
37	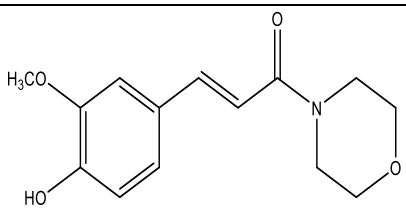	**38**	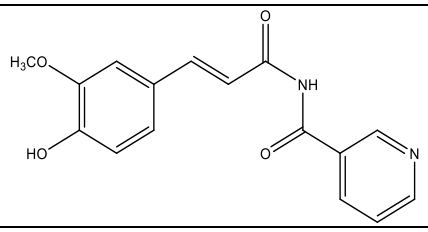

Table 2 Antibacterial data of ferulic acid derivatives used in QSAR studies.

C. No.	$pMIC_{EC}$	$pMIC_{SA}$	$pMIC_{BS}$	C. No.	$pMIC_{EC}$	$pMIC_{SA}$	$pMIC_{BS}$
1	1.06	1.96	1.96	**20**	1.36	1.06	1.36
2	1.72	1.11	1.41	**21**	1.38	1.08	1.38
3	1.35	1.35	1.35	**22**	1.38	1.08	1.38
4	1.30	1.30	1.30	**23**	1.38	1.08	1.38
5	1.28	1.28	1.28	**24**	1.38	1.08	1.38
6	1.36	1.36	1.66	**25**	1.40	1.10	1.10
7	0.80	1.10	1.40	**26**	1.40	1.10	1.40
8	1.72	1.42	1.42	**27**	1.40	1.10	1.70
9	1.22	1.22	0.92	**28**	1.06	1.06	1.36
10	1.33	1.33	1.33	**29**	1.11	1.11	1.41
11	1.30	1.30	1.00	**30**	1.36	1.06	1.36
12	1.25	1.25	0.95	**31**	1.38	1.08	1.38
13	0.67	0.97	0.97	**32**	1.36	1.06	1.36
14	1.34	1.34	1.34	**33**	1.36	1.06	1.36
15	1.03	1.03	1.34	**34**	1.41	1.11	1.41
16	1.12	1.12	1.42	**35**	1.28	0.97	1.28
17	1.14	1.14	1.44	**36**	1.89	1.00	1.30
18	1.08	1.08	1.39	**37**	1.92	1.02	1.32
19	1.08	1.08	1.39	**38**	1.68	1.08	1.38

Calculation of Molecular Descriptors

Various molecular descriptors such as Randic topological index (R), molar refractivity (MR), log P (octanol-water partition coefficient), valence molecular connectivity indices ($^0\chi^V$, $^1\chi^V$, $^2\chi^V$, $^3\chi^V$), and Kier's shape indices ($k\alpha^1$, $k\alpha^2$, $k\alpha^3$), Total energy (TE), Wiener topological index (W), Balaban topological index (J), lowest unoccupied molecular orbital (LUMO) and energies of highest occupied molecular orbital (HOMO), electronic energy and dipole moment (μ) of ferulic acid derivatives (1-38) were calculated (**Table 3**) using **TSAR 3.3.** [28-33].

Table 3 Selected molecular descriptors of ferulic acid derivatives

C. No.	μ	log P	MR	$^1\chi$	$^1\chi^v$	$^3\chi^v$	κ^1	$\kappa\alpha^3$	J	LUMO
1	1.79	2.55	80.46	10.08	6.21	0.43	17.36	4.34	1.52	-0.74
2	2.34	3.42	89.69	11.67	7.28	0.47	18.78	3.91	1.29	-0.75
3	0.49	3.23	77.00	9.69	6.95	0.39	16.37	4.54	1.51	-0.69
4	0.51	2.86	69.86	8.67	5.89	0.27	16.06	5.15	2.02	-0.72
5	0.46	2.40	65.15	8.02	5.28	0.50	15.06	4.48	2.08	-0.70
6	0.78	3.42	80.60	10.19	6.45	0.39	17.36	4.65	1.48	-0.72
7	4.07	3.28	83.09	10.99	6.51	0.45	19.33	4.63	1.53	-1.23
8	0.49	4.69	95.17	11.40	8.66	1.12	20.31	5.26	1.64	-0.70
9	0.67	1.65	55.99	7.17	4.30	0.27	13.07	3.28	2.07	-0.75
10	0.50	3.19	74.41	9.02	6.24	0.68	17.05	5.79	2.03	-0.72
11	0.56	2.86	69.73	8.52	5.74	0.68	16.06	5.15	2.06	-0.73
12	0.49	1.99	60.73	7.67	4.89	0.27	14.06	3.89	2.06	-0.72
13	0.53	2.46	65.26	8.17	5.39	0.27	15.06	4.48	2.04	-0.72
14	0.57	3.33	75.76	9.69	6.01	0.34	16.37	4.12	1.51	-0.83
15	4.23	2.68	77.71	9.69	6.10	0.36	16.37	4.12	1.51	-0.70
16	5.55	3.10	90.08	11.40	7.02	0.61	20.31	4.64	1.60	-1.00
17	0.72	3.15	89.84	11.40	7.11	0.64	20.31	4.79	1.58	-1.28
18	4.34	3.20	82.52	10.08	6.61	0.56	17.36	4.51	1.51	-0.79
19	4.81	3.20	82.52	10.10	6.61	0.52	17.36	4.24	1.55	-0.77
20	4.33	3.15	82.75	10.08	6.51	0.53	17.36	4.36	1.51	-0.70
21	5.46	2.43	84.18	10.63	6.63	0.41	18.34	4.34	1.58	-0.64
22	4.41	3.61	87.80	10.51	6.93	0.62	18.34	4.12	1.56	-0.69
23	4.46	3.61	87.80	10.49	6.93	0.66	18.34	4.36	1.56	-0.69
24	4.35	3.61	87.80	10.49	6.93	0.66	18.34	4.36	1.57	-0.69
25	5.74	2.63	85.04	11.01	6.60	0.45	19.33	4.38	1.62	-1.10
26	1.71	2.63	85.04	10.99	6.60	0.47	19.33	4.63	1.53	-1.16
27	5.44	2.63	85.04	10.99	6.60	0.47	19.33	4.63	1.52	-1.01

28	4.28	3.15	82.75	10.10	6.52	0.50	17.36	4.10	1.55	-0.70
29	1.83	3.34	82.73	10.49	6.71	0.59	18.34	4.47	1.53	-0.87
30	4.35	3.15	82.75	10.08	6.51	0.53	17.36	4.36	1.52	-0.69
31	4.71	2.43	84.18	10.62	6.62	0.43	18.34	4.60	1.51	-0.70
32	4.78	2.82	77.93	10.10	6.21	0.41	17.36	4.06	1.55	-0.75
33	1.21	2.77	82.55	10.19	6.56	0.40	17.36	4.65	1.48	-0.56
34	4.35	3.68	94.16	11.65	7.50	0.53	18.78	3.96	1.24	-0.64
35	1.40	1.81	67.21	8.17	5.50	0.28	15.06	4.48	2.04	-0.53
36	1.40	2.21	71.81	8.67	6.00	0.28	16.06	5.15	2.02	-0.53
37	1.71	0.90	71.91	9.20	6.12	0.38	15.39	3.71	1.55	-0.57
38	5.36	1.82	80.59	10.60	6.40	0.41	18.34	4.62	1.54	-0.85

QSAR Model Development

The QSAR equation by linear/ multiple linear regression analysis was developed using **SPSS 28.0 trial version.** By evaluating actual and estimated values, the QSAR models were found to be accurate, calculating q2 (LOO method) and detecting systemic error.

Molecular Docking Study

The ferulic acid derivatives (1-38) **Table 1,** selected from the reported work by Khatkar et al. (2015,) were sketched using **ChemDraw 19.0.** The molecular docking was done using **Schrodinger suite v 13.1.**

Protein Preparation

Transcriptional regulation (**PDB Id: 5X14**) was picked from the Protein Data Bank for the molecular docking research of a selected data set of ferulic acid derivatives. The average PDB structure file for molecular modelling calculations needs to be more suitable. Heavy-weight atoms, cofactors, water particles, co-crystallized ligands and metal ions are all found in a typical PDB structure file. The protein preparation wizard was used to construct the protein, which was preprocessed, optimised, and reduced. The final result is a refined, hydrogenated ligand and ligand-receptor complex structure that can be used with various Schrodinger modules [34].

Ligand Preparation

Ligands were prepared using the ***maestro v13.1*** LigPrep module for the best docking outcomes. The structures to be docked must be close to the ligand as they would appear in a protein-ligand complex. This means that the structures must obey the specifications of the Glide docking program. They should possess a 3-D appearance. Glide-only modified torsional coordinates of ligands and geometric parameters should be changed before use. A single molecule should be present in them that would not be connected with any receptor or other components. They should have a suitable system of protonation that would be appropriate for biological pH levels (~ 7) [35, 36].

Grid Generation

The receptor grid generating module of ***maestro version 13.1*** created the grid. A grid was built near the docking site previously engaged by the co-crystallized ligand, allowing additional molecules to be bound to the similar docking site. In contrast, the co-crystallized ligand was excluded [37].

Molecular Docking

Docking was done by using ***maestro v 13.1.*** The XP module performs more precise molecular docking of chosen ferulic acid molecules. At each level, the collected data's size shrinks as the data's precision expands. In ***maestro v 13.1,*** XP parameters (glide energy, glide e-model value, docking score) were calculated [38, 39].

ADME Study

Most pharmacological compounds fail during clinical trials, and determining ADME features is critical. **QikProp, GLIDE,** and **Schrodinger v 13.1** were used to determine the likeliness and ADME attributes of the most active compounds. The ligand was prepared in Maestro format (.maez) for ADME investigation using the LigPrep module of **Schrodinger v 13.1.** Then we got down to business, navigated the QikPro dialogue box, and inserted the synthesised derivatives' ligand preparation file (**.maez**) to get the ADME parameters [40].

Molecular Dynamics Simulation

Any grid-based docking approach has the drawback of treating the receptor as a rigid entity, resulting in a static image of the protein-ligand interaction. In the physiological system, however, this relationship is dynamic MD simulations were performed for 10ns using the System builder panel in Desmond suit of Schrodinger 13.1 (Academic version) using OPLS4 force field [41]. The SPC (simple point charge) water box and orthorhombic boundaries were applied to the system. The plan was neutralised by adding Na+ as counter ions [42,

43]. Further, the molecular dynamics panel of Desmond was used to run simulation calculations by adjusting simulation time, ensemble class, simple model system before simulation etc. All the default functions were used to run the estimates [44]. The simulation results were analysed by RMSD (Root Mean Square Deviation) and RMSF (Root Mean Square Fluctuations), Protein-ligand interaction and contacts [45].

RESULTS AND DISCUSSION

2D QSAR Study

In response to the initial findings, and as part of our ongoing work using Hansch analysis on the association of biological activities with different molecular structures [46], we provide here the QSAR investigations of ferulic acid derivatives synthesised by Khatkar *et al.*, (2015). In this study, the structure l features of the drug molecules were first quantified using various molecular descriptors (**Table 3**). Then the use of characteristics and biological activity was quantified and correlated to equations using linear/ multiple linear regression. Biological data determined as MIC values were first changed into the pMIC values (**Table 2**) and used as the dependent variable in the QSAR study.

QSAR models for antibacterial potential against *Escherichia Coli* are as follows

The initial study was done using correlation analysis. The correlation matrix generated for ferulic acid antibacterial effectiveness against ***Escherichia Coli*** is shown in Table 4. There was much colinearity (r > 0.8) between various parameters. In defining the antibacterial action of ferulic acid derivatives, the correlation matrix revealed that the electronic parameter **Vamp Lumo (r = 0.330, Eq. 1) Table 4.**

The equation comes out as:

$$pMIC_{ec} = -0.466\ VAMP\ LUMO - 1.675 \quad (Eq.1)$$

$$n= 38,\ r= 0.330,\ q^2= -0.002,\ F= 0.042,\ SD= 0.240$$

where q^2 - cross-validated, n - number of data points, F - Fischer statistics, r - correlation coefficients, r^2 - obtained by leaving one out method, SD - standard deviation

For improvement of the r value, valuence first-order molecular connectivity indices were added to Vamp Lumo, which enhanced the correlation value to 0.465, (Eq. 2).

$$pMIC_{ec} = -0.112\ VAMP\ LUMO - 0.547\,{}^1\chi^V - 1.018 \quad (Eq.\ 2)$$

$$n= 38,\ r= 0.465,\ q^2= 0.079,\ F= 0.013,\ SD= 0.228$$

For further improvement of the r value, Log P was added in Eq. 2, which enhanced the correlation value to 0.652, (Eq. 3).

$$pMIC_{ec} = 0.242\ VAMP\ LUMO - 0.273\ {}^1\chi^V - 0.530\ Log\ P - 0.665 \quad (Eq.3)$$

$$n= 38,\ r= 0.652,\ q^2= 0.283,\ F= 0.000,\ SD= 0.198$$

But as the value of r is not closer to 1, and the value of q^2 is also not near 0.5 or above, this indicates that the model is not significant. This may be due to the presence of outliers. Therefore 11 outliers (compound 36, 35, 28, 21, 15, 14, 13, 9, 8, 2, 1) were identified and removed, which improved the value of r to 0.824 (Eq. 4). The equation is statistically significant.

$$pMIC_{ec} = 0.271\ VAMP\ LUMO - 0.188\ {}^1\chi^V - 0.519\ Log\ P - 1.304 \quad (Eq.4)$$

$$n= 27,\ r= 0.824,\ q^2= 0.578,\ F= 3.598,\ SD= 0.120$$

Table 4: Correlation matrix for antibacterial activity against Escherichia *Coli*

	$pMIC_{EC}$	μ	log P	MR	${}^1\chi$	${}^1\chi^v$	${}^3\chi^v$	κ^1	$\kappa\alpha^3$	J	LUMO
$pMIC_{EC}$	1.00										
μ	0.03	1.00									
log P	0.13	0.10	1.00								
MR	-0.15	0.54	0.67	1.00							
${}^1\chi$	-0.13	0.56	0.57	0.97	1.00						
${}^1\chi^v$	-0.27	0.34	0.73	0.94	0.88	1.00					
${}^3\chi^v$	-0.13	0.11	0.70	0.62	0.50	0.71	1.00				
κ^1	-0.08	0.51	0.58	0.93	0.95	0.86	0.61	1.00			
$\kappa\alpha^3$	-0.06	-0.24	0.30	0.14	0.08	0.27	0.39	0.30	1.00		
J	0.12	-0.54	-0.41	-0.81	-0.85	-0.70	-0.23	-0.66	0.28	1.00	
LUMO	-0.33	-0.17	-0.14	-0.30	-0.44	-0.17	-0.15	-0.55	-0.12	0.20	1.00

More than 0.5 value of q2 showed that the QSAR model is valid. In contrast, the validity of the

QSAR model is demonstrated by plotting observed against predicted activity (**Figure 1; Table 4**). The observed values were plotted against residual values to calculate the systemic error (**Figure 2**). The zero residual propagation on every dimension demonstrated the absence of systemic error in creating the QSAR model.

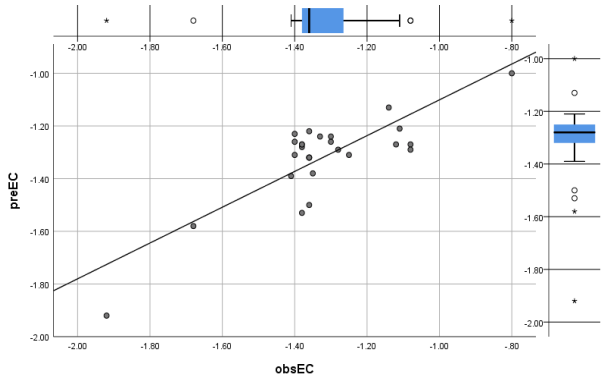

Fig. 1 Plot of Observed vs. Predicted Activity

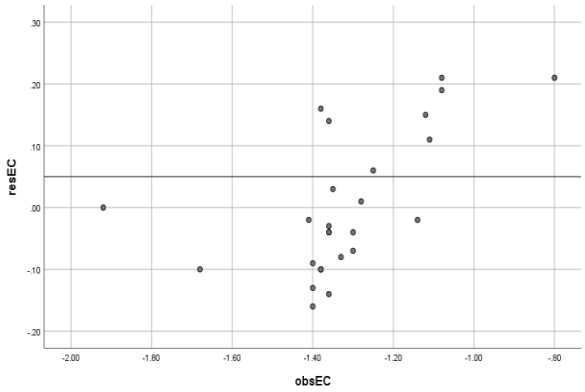

Fig. 2 Comparison of Observed vs. Residual Activity

QSAR models for antibacterial activity against *Staphylococcus aureus* are as follows

The Preliminary investigation was done using the correlation of molecular descriptors with the antibacterial potential of ***Staphylococcus aureus.*** The initial correlation of **r = 0.437** was observed with the electronic parameter **Total dipole (Eq. 5) Table 5,** which is insignificant.

The equation comes out as:

$$pMIC_{sa} = 0.039\ \mu - 1.266 \quad (\text{Eq. } 5)$$

n= 38, r= 0.437, q^2= 0.122, F= 0.005, SD= 0.161

For further improvement of r value, valence third-order molecular connectivity indices was added to a total dipole, which enhanced the correlation digits to 0.481, (Eq. 6).

$$pMIC_{sa} = 0.041\ \mu - 0.219\ {}^{3}\chi^{V} - 1.167 \quad (\text{Eq. } 6)$$

n= 38, r= 0.481, q^2= 0.128, F= 0.009, SD= 0.160

But as the value of r is not closer to 1, and the value of q^2 is also not near 0.5 or above, this indicates that the model is not significant. This may be due to the presence of outliers. Therefore 9 outliers (compound 37, 36, 35, 33, 29, 17, 13, 6, and 1) were identified and removed, which improved the value of r to 0.896 (Eq. 7). The equation is statistically significant.

$$pMIC_{sa} = 0.049\ \mu - 0.128\ {}^{3}\chi^{V} - 1.246 \quad (\text{Eq. } 7)$$

n= 29, r= 0.896, q^2= 0.716, F= 3.041, SD= 0.052

Table 5: Correlation matrix for antibacterial activity again Staphylococcus aureus

	$pMIC_{SA}$	**μ**	**log P**	**MR**	**${}^{1}\chi$**	**${}^{1}\chi^{v}$**	**${}^{3}\chi^{v}$**	**κ^{1}**	**$\kappa\alpha^{3}$**	**J**	**LUMO**
$pMIC_{SA}$	1.00										
μ	0.44	1.00									
log P	-0.17	0.10	1.00								
MR	0.08	0.54	0.67	1.00							
${}^{1}\chi$	0.09	0.56	0.57	0.97	1.00						
${}^{1}\chi^{v}$	0.01	0.34	0.73	0.94	0.88	1.00					
${}^{3}\chi^{v}$	-0.15	0.11	0.70	0.62	0.50	0.71	1.00				
κ^{1}	0.06	0.51	0.58	0.93	0.95	0.86	0.61	1.00			
$\kappa\alpha^{3}$	-0.19	-0.24	0.30	0.14	0.08	0.27	0.39	0.30	1.00		
J	-0.08	-0.54	-0.41	-0.81	-0.85	-0.70	-0.23	-0.66	0.28	1.00	
LUMO	0.01	-0.17	-0.14	-0.30	-0.44	-0.17	-0.15	-0.55	-0.12	0.20	1.00

More than 0.5 value of q2 showed that the QSAR model is valid. In contrast, the validity of the QSAR model is demonstrated by plotting observed against predicted activity (**Figure 3; Table 5**). The observed values were plotted against residual values to calculate the systemic error (**Figure 4**). The zero residual propagation on both sides demonstrated the absence of systemic error in creating the QSAR model.

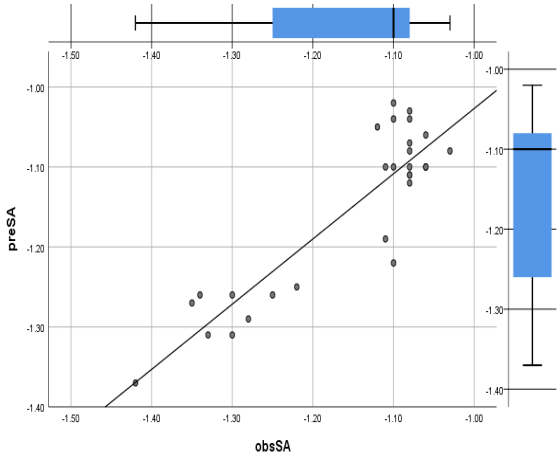

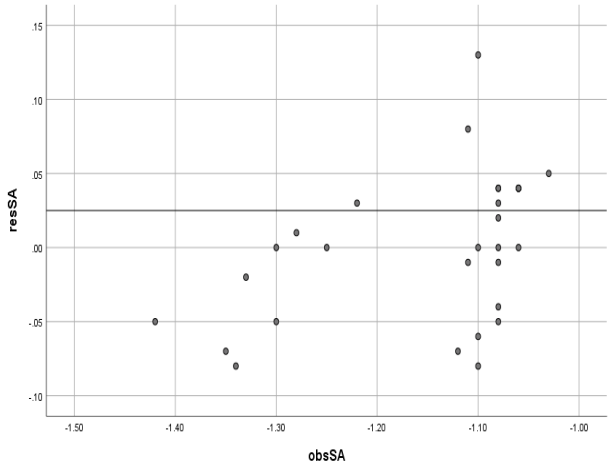

Fig. 3 Comparison of Observed vs. Predicted Activity **Fig. 4** Comparison of Observed vs. Residual Activity

QSAR models for antibacterial activity against *Bacillus subtilis* are as follows

The Preliminary investigation was carried out in terms of the correlation of molecular descriptors with the antibacterial activity of ***Bacillus subtilis.*** The initial correlation of **r = 0.610** was seen with the topological parameter **Balaban (Eq. 8) Table 6,** which is insignificant.

The equation comes out as:

$$pMIC_{bs} = 0.486\ J - 2.148 \quad (\text{Eq. } 8)$$

n= 38, r= 0.610, q^2= 0.291, F= 4.454, SD= 0.151

For further improvement of the r value, kier's third-order alpha shape indices were added to Balaban, which enhanced the correlation value to 0.703, (Eq. 9).

$$pMIC_{bs} = -0.133\ J + 0.500\ K\alpha^3 - 1.423 \quad (\text{Eq. } 9)$$

n= 38, r= 0.703, q^2= 0.426, F= 5.328, SD= 0.137

But as the value of r is not closer to 1, and the value of q^2 is also not near 0.5 or above, this indicates that the model is not significant. This may be due to the presence of outliers. Therefore 8 outliers (compound 35, 33, 27, 25, 13, 11, 13, 1) were identified and removed, which increased the value of r to 0.879 (Eq. 10). The equation is statistically significant.

$$pMIC_{bs} = -0.142\ J + 0.398\ K\alpha^3 - 1.205 \quad (\text{Eq. } 10)$$

n= 30, r= 0.879, q^2= 0.694, F= 4.468, SD= 0.063

Table 6: Correlation matrix for antibacterial activity against *Bacillus subtilis*

	$pMIC_{BS}$	μ	log P	MR	$^1\chi$	$^1\chi^v$	$^3\chi^v$	κ^1	$\kappa\alpha^3$	J	LUMO
$pMIC_{BS}$	1.00										
μ	-0.24	1.00									
log P	-0.31	0.10	1.00								
MR	-0.59	0.54	0.67	1.00							
$^1\chi$	-0.59	0.56	0.57	0.97	1.00						
$^1\chi^v$	-0.52	0.34	0.73	0.94	0.88	1.00					
$^3\chi^v$	-0.23	0.11	0.70	0.62	0.50	0.71	1.00				
κ^1	-0.54	0.51	0.58	0.93	0.95	0.86	0.61	1.00			
$\kappa\alpha^3$	-0.16	-0.24	0.30	0.14	0.08	0.27	0.39	0.30	1.00		
J	0.61	-0.54	-0.41	-0.81	-0.85	-0.70	-0.23	-0.66	0.28	1.00	
LUMO	0.12	-0.17	-0.14	-0.30	-0.44	-0.17	-0.15	-0.55	-0.12	0.20	1.00

More than 0.5 value of q2 showed that the QSAR model is valid. In contrast, the validity of the QSAR model is demonstrated by plotting observed against predicted activity (**Figure 5; Table 6**). The observed values were plotted against residual values to calculate the systemic error (Figure 6). The zero residual propagation on both sides demonstrated the absence of systemic error in creating the QSAR model.

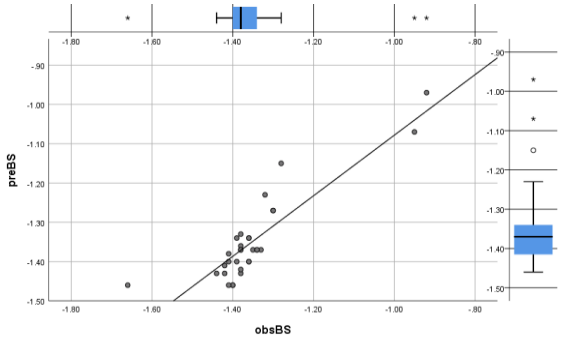

Fig. 5 Comparison of Observed vs. Predicted Activity

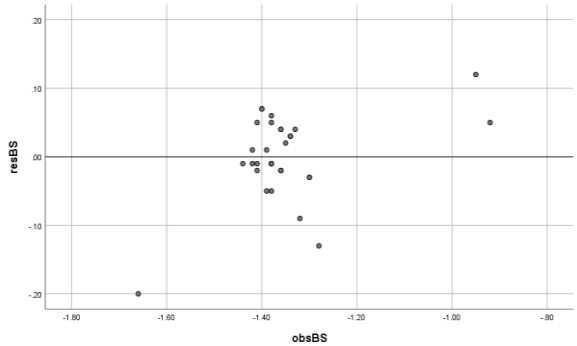

Fig. 6 Comparison of Observed vs. Residual Activity

We can conclude From the above data that all QSAR models are valid. In contrast, the validity of the QSAR model is demonstrated by the comparison of observed, predicted, and residual values of each of the organisms taken, shown in **Table 7.**

Table 7: Observed, predicted, and residual activity values of the ferulic acid derivatives

C. No.	*Escherichia Coli*			*Staphylococcus aureus*			*Bacillus subtilis*		
	Obs.	**Pre.**	**Res.**	**Obs.**	**Pre.**	**Res.**	**Obs.**	**Pre.**	**Res.**
1	-	-	-	-	-	-	-	-	-
2	-	-	-	-1.11	-1.19	0.08	-1.41	-1.40	-0.01
3	-1.35	-1.38	0.03	-1.35	-1.27	-0.07	-1.35	-1.37	0.02
4	-1.30	-1.26	-0.04	-1.30	-1.26	-0.05	-1.30	-1.27	-0.03
5	-1.28	-1.29	0.01	-1.28	-1.29	0.01	-1.28	-1.15	-0.13
6	-1.36	-1.22	-0.14	-	-	-	-1.66	-1.46	-0.20
7	-0.80	-1.00	0.21	-1.11	-1.19	0.08	-1.40	-1.46	0.07
8	-	-	-	-1.35	-1.27	-0.07	-1.42	-1.41	-0.01
9	-	-	-	-1.30	-1.26	-0.05	-0.92	-0.97	0.05
10	-1.33	-1.24	-0.08	-1.28	-1.29	0.01	-1.33	-1.37	0.04
11	-1.30	-1.24	-0.07	-1.30	-1.31	0.00	-	-	-
12	-1.25	-1.31	0.06	-1.25	-1.26	0.00	-0.95	-1.07	0.12
13	-	-	-	-	-	-	-	-	-
14	-	-	-	-1.34	-1.26	-0.08	-1.34	-1.37	0.03
15	-	-	-	-1.03	-1.08	0.05	-1.34	-1.37	0.03
16	-1.12	-1.27	0.15	-1.12	-1.05	-0.07	-1.42	-1.43	0.01
17	-1.14	-1.13	-0.02	-	-	-	-1.44	-1.43	-0.01
18	-1.08	-1.27	0.19	-1.08	-1.10	0.02	-1.39	-1.40	0.01
19	-1.08	-1.29	0.21	-1.08	-1.08	0.00	-1.39	-1.34	-0.05
20	-1.36	-1.32	-0.04	-1.06	-1.10	0.04	-1.36	-1.40	0.04
21	-	-	-	-1.08	-1.03	-0.05	-1.38	-1.36	-0.01
22	-1.38	-1.28	-0.10	-1.08	-1.11	0.03	-1.38	-1.33	-0.05
23	-1.38	-1.27	-0.10	-1.08	-1.11	0.04	-1.38	-1.37	-0.01
24	-1.38	-1.27	-0.10	-1.08	-1.12	0.04	-1.38	-1.37	-0.01
25	-1.40	-1.26	-0.13	-1.10	-1.02	-0.08	-	-	-
26	-1.40	-1.23	-0.16	-1.10	-1.22	0.13	-1.40	-1.46	0.07
27	-1.40	-1.31	-0.09	-1.10	-1.04	-0.06	-	-	-
28	-	-	-	-1.06	-1.10	0.04	-1.36	-1.34	-0.02
29	-1.11	-1.21	0.11	-	-	-	-1.41	-1.38	-0.02
30	-1.36	-1.32	-0.04	-1.06	-1.10	0.04	-1.36	-1.40	0.04
31	-1.38	-1.53	0.16	-1.08	-1.07	-0.01	-1.38	-1.43	0.06
32	-1.36	-1.32	-0.03	-1.06	-1.06	0.00	-1.36	-1.34	-0.02
33	-1.36	-1.50	0.14	-	-	-	-	-	-
34	-1.41	-1.39	-0.02	-1.11	-1.10	-0.01	-1.41	-1.46	0.05
35	-	-	-	-	-	-	-	-	-
36	-	-	-	-	-	-	-1.30	-1.27	-0.03
37	-1.92	-1.92	0.00	-	-	-	-1.32	-1.23	-0.09
38	-1.68	-1.58	-0.10	-1.08	-1.04	-0.04	-1.38	-1.42	0.05

Note: (-) used in the table refers to the outliers removed against the particular organisms.

Molecular Docking

The Ferulic acid derivatives were selected from reported work by Khatkar et al., (2015) (**Table 2**), and their antibacterial docking score was determined by molecular docking software **Schrodinger v 13.1, using PDB: 5X14 (Table 8)** concerning a standard drug **(norfloxacin).**

Table 8 Docking score and Glide energy of the ferulic acid derivatives

C. No.	Docking score	Glide energy	C. No.	Docking score	Glide energy
1	-6.559	-30.823	**21**	-7.050	-34.059
2	-5.540	-41.275	**22**	-6.423	-30.077
3	-6.426	-28.032	**23**	-6.919	-32.541
4	-6.564	-38.243	**24**	-6.855	-32.460
5	-6.569	-36.904	**25**	-6.852	-34.200
6	-6.788	-31.130	**26**	-6.963	-34.181
7	-4.991	-38.558	**27**	-4.327	-34.234
8	-6.996	-31.665	**28**	-6.737	-30.749
9	-6.660	-37.154	**29**	-6.848	-30.370
10	-6.618	-39.711	**30**	-7.005	-32.583
11	-6.665	-37.149	**31**	-6.693	-33.618
12	-6.670	-38.220	**32**	-7.009	-30.414
13	-6.703	-36.643	**33**	-6.531	-33.502
14	-5.916	-37.437	**34**	-6.774	-34.655
15	-7.243	-30.786	**35**	-6.525	-36.196
16	-6.733	-34.619	**36**	-6.295	-28.659
17	-6.586	-32.915	**37**	-6.238	-30.660
18	-7.424	-32.335	**38**	-6.362	-36.512
19	-6.691	-32.405	**Norfloxacin**	-4.555	-31.366
20	-6.935	-32.804	**Ferulic acid**	-7.620	-35.374

The binding mechanism of the ferulic acid derivatives with their respective receptors was investigated using molecular docking. The active site of transcriptional regulation (**PDB ID: 5X14**) was used to conduct a molecular docking investigation of ferulic acid compounds and a conventional medication (**norfloxacin**). The oxygen atom of compound **18**'s amide nucleus made hydrogen bonds with Arg164, Hie154, and water amino acid residues, according to the 2-D ligand interaction diagrammatic perspective. Hie154 and water amino acid residues made hydrogen bonds with the oxygen atoms of compounds **15** and **21**'s amide nucleus. Hie154 and water amino acid residues made hydrogen bonds with the oxygen atoms of the amide nucleus of compounds **32** and **30.** The docking scores glide energy and e-model values were shown in negative terms. The lower the docking score, the better the ligand's affinity for binding to the receptor. Table 9 shows the docking data for the top five compounds (**18, 15, 21, 32 and 30**) and the reference medication. Figures **7, 8, 9, 10, 11**, and **12** illustrate the ligand interaction diagram and the binding surface of docked molecules **18, 15, 21, 32, 30**, and **norfloxacin**, respectively. By interacting with homologous amino acid residues, these molecules have the same homology as normal norfloxacin, according to the 2-D ligand interaction diagrammatic perspective.

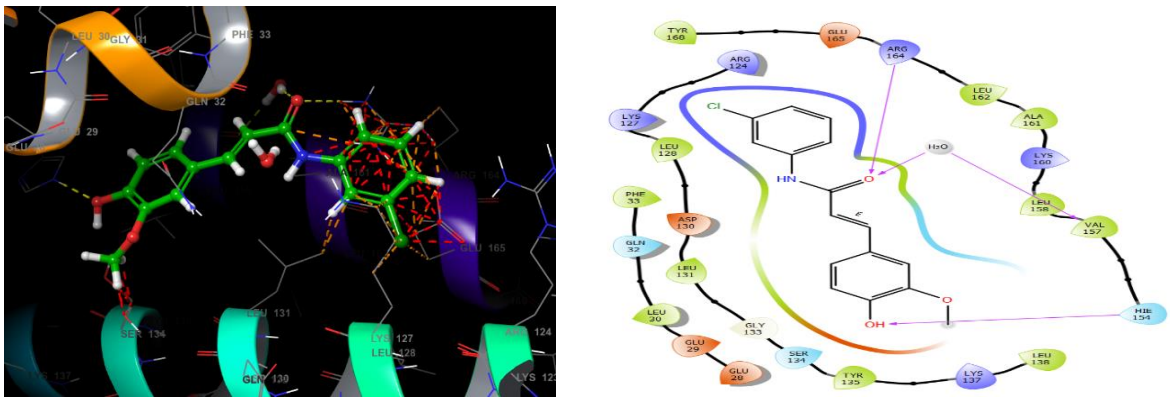

Fig. 7: Binding surface and 2D interaction of molecule 18

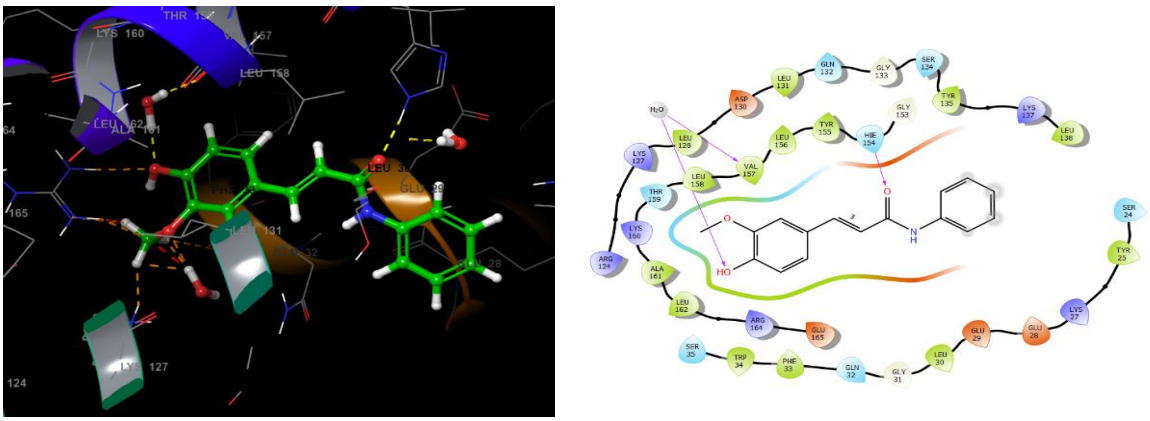

Fig. 8: Binding surface and 2D interaction of molecule 15

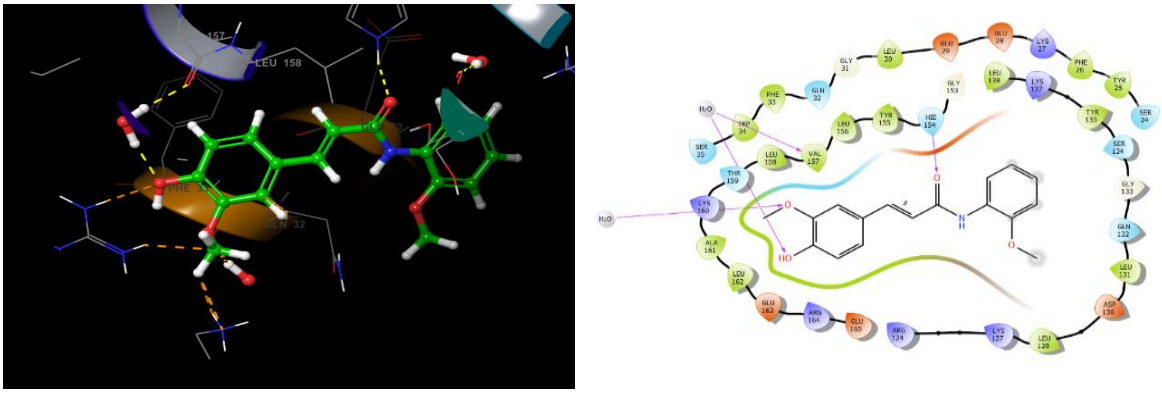

Fig. 9: Binding surface and 2D interaction of molecule 21

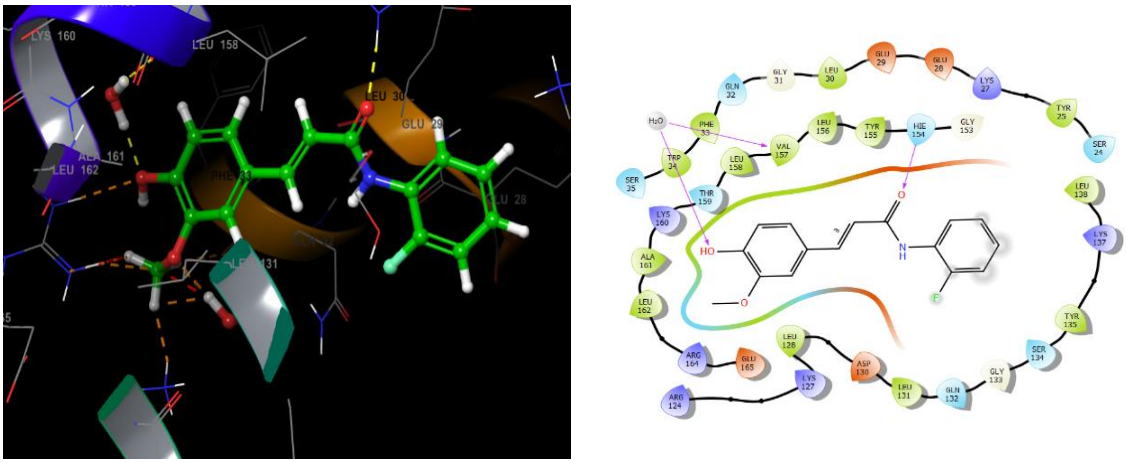

Fig. 10: Binding surface and 2D interaction of molecule 32

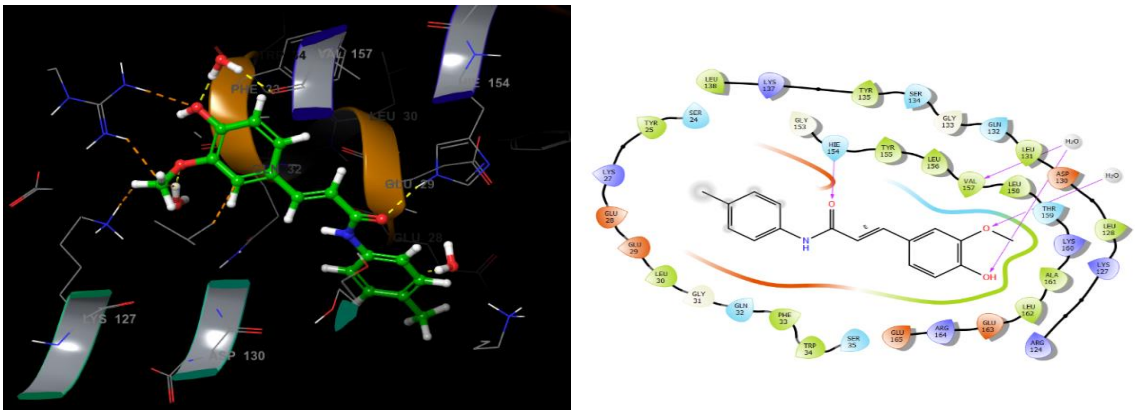

Fig. 11: Binding surface and 2D interaction of molecule 30

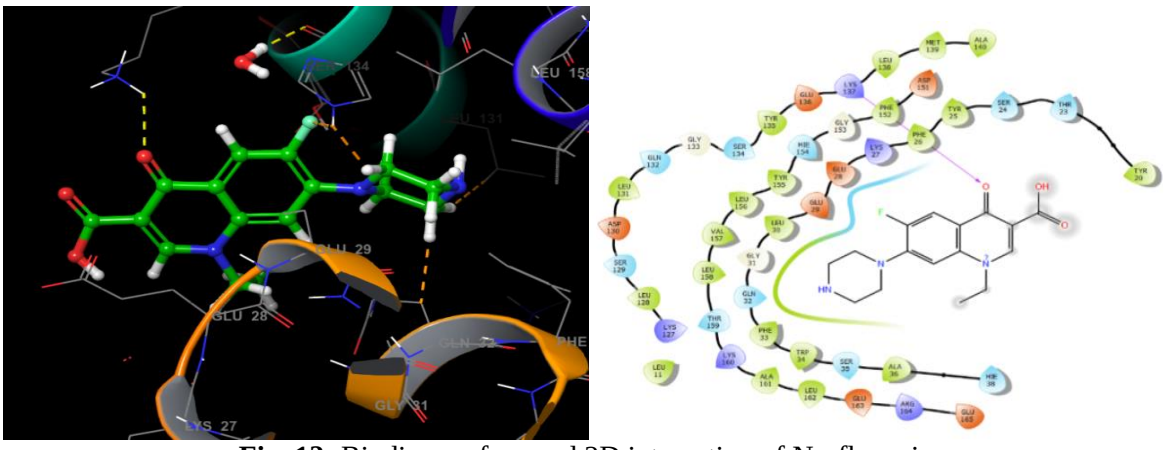

Fig. 12: Binding surface and 2D interaction of Norfloxacin

Table 9: Docking score of the top five ferulic acid derivatives

C. No.	Docking score	Glide energy	Glide emodel	Interacting residues
18	-7.424	-32.335	-47.525	Glu29, Glu32, Phe33, Leu131, Leu158, Val157, Hie154, Ala161, Ser134, Arg164, Lys127, Lys137, Glu28
15	-7.243	-30.786	-38.484	Glu29, Glu32, Phe33, Leu131, Leu158, Val157, Hie154, Ala161, Ser134, Arg164, Lys127, Lys137, Glu28
21	-7.050	-34.059	-50.763	Glu29, Glu32, Phe33, Leu131, Leu158, Val157, Hie154, Ala161, Ser134, Arg164, Lys127, Lys137, Glu28, Lys27, Glu165
32	-7.009	-30.414	-42.981	Glu29, Glu32, Phe33, Leu131, Leu158, Val157, Hie154, Ala161, Ser134, Arg164, Lys127, Lys137, Glu28
30	-7.005	-32.583	-39.353	Glu29, Glu32, Phe33, Leu131, Leu158, Val157, Hie154, Ala161, Ser134, Arg164, Lys127, Lys137, Glu28, Glu165
Norfloxacin	-4.555	-31.366	-36.099	Glu29, Glu32, Phe33, Leu131, Leu158, Val157, Hie154, Ala161, Ser134, Lys127, Lys137, Glu28

ADME Study

The ADME characteristics of the presented ferulic acid derivatives were determined using the **Schrodinger v 13.1 QikProp module. Table 10** summarises ADMET data of the best active complexes, namely **18, 15, 21, 32,** and **30**. All of the considerations of the Lipinski rule of five were followed by the molecules **18, 15, 21, 32,** and **30**. The results showed that compounds **18, 15, 21, 32**, and **30** follow Lipinski's rule, indicating that these derivatives could be used as prototype molecules for advanced research.

Table 10: ADME data of most active compounds calculates using Qik Prop Simulation

C.No.	MW	QPlogPo/w	AcceptHB	QPlogBB	DonorHB	Human oral absorption	Rule of Five
15	269.2	2.9	4	-0.8	2	3	0
18	303.7	3.3	4	-0.6	2	3	0
21	299.3	3.0	4.75	-0.8	2	3	0
30	283.3	3.2	4	-0.8	2	3	0
32	287.2	3.1	4	-0.7	2	3	0

✓Molecular weight, not more than 500 Da.
✓Hydrogen bond donor (Accepted Limit: ≤ 5)
✓Hydrogen bond acceptor (Accepted Limit: ≤ 10)
✓Log P less than 5.
✓Human oral absorption – 1, 2, or 3 for low, medium, or high.
✓QPlogBB range from -3.0 to 1.2.

Molecular Dynamics Simulation

Molecular dynamics simulations were performed for compounds 18 and 21 based on their biological activity, i.e., pMIC values and molecular docking with Transcriptional regulation (5X14). Compound 18 showed protein RMSD values in the series of (4 - 6) Å and ligand RMSD values in the range of (4 - 7) Å with fluctuations at various time intervals. The

RMSD graph tells us the stability of the protein-ligand complex, which is verified that the lesser the RMSD greater the stability (**Fig. 13(a)**). The RMSF value lies in (1.5- 8.8) Å. The RMSF graph depicts the mobility of target proteins, with frequent peaks showing the presence of flexible amino acids on the C-alpha backbone of the protein (**Fig. 13(b)**). MD simulation outcomes specify probable protein-ligand interactions in the form of histograms and heat maps (**Fig. 13(c), (d)**). The interface between protein and ligand comprises four types of bonds, hydrogen bonds (green), hydrophobic interaction (grey), ionic bonds (pink), and water bridges (blue). The amino acids residues Arg13, Glu29, Ser134, His154, and Arg164 forms hydrogen bonds (green), Leu30, Phe33, Trp34, Lys127, Leu131, His154, Val157, Leu158, Ala161, and Arg164 form hydrophobic interaction (grey), and Ala7, Gly10, Arg13, Leu11, Glu28, Glu29, Gln32, Lys127, Asp130, Ser134, Lys 137, Gly 153, His154, Val157, Ala161, Arg164 forms water bridges (blue) respectively (**Fig. 13 (c)**). The residue Arg164 showed 33% interaction more than 30% of the time by forming a water bridge with the ligand molecules (**Fig. 13 (d)**).

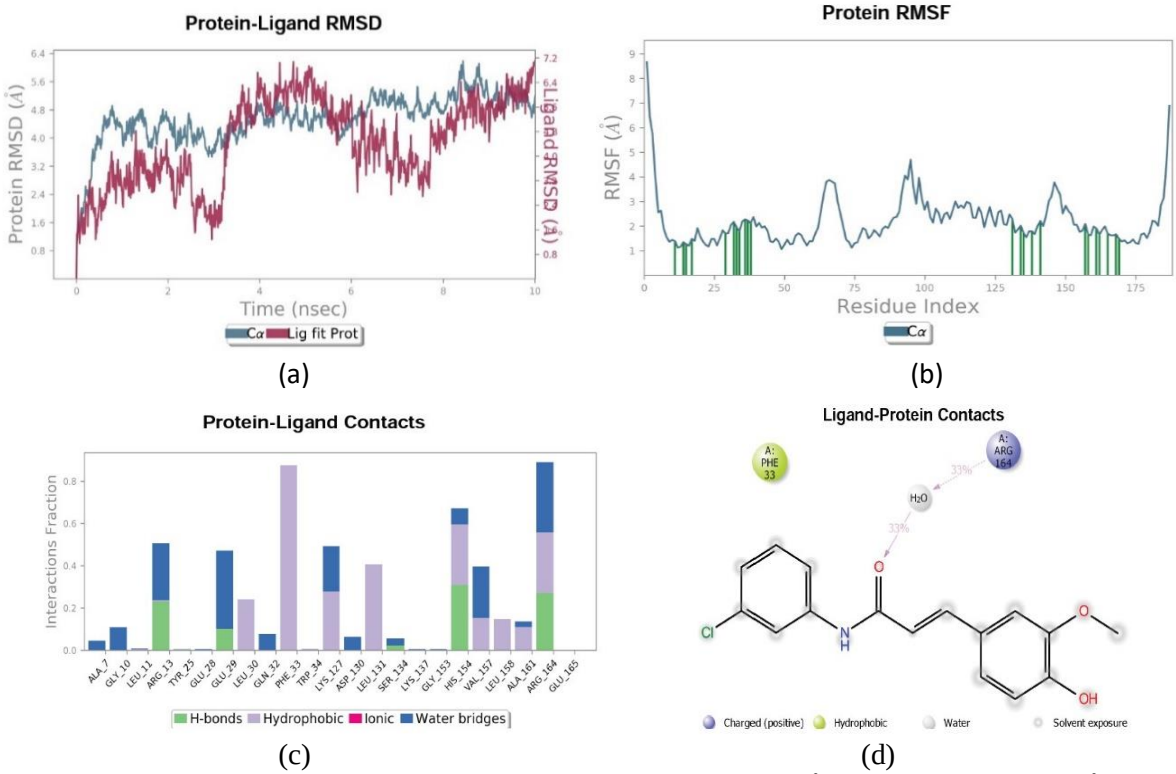

Fig. 13: Compound 18 (a) Graphical representation of Protein RMSD (Å) and Ligand RMSD (Å) versus time (ns), (b) Graphical representation of RMSF (Å) versus the residual index, (c) Histogram representation specify probable protein-ligand interactions, (d) Ligand protein contact.

Compound 21 showed protein RMSD values in the range of (4-5.5) Å and ligand RMSD values in the range of (4-7.5) Å with fluctuations at various time intervals. The RMSD graph tells us the stability of the protein-ligand complex, which is verified that the lesser the RMSD greater the stability (**Fig. 13(a)**). The RMSF value lies in the range of (1.4-7.4) Å. The RMSF graph depicts the mobility of target proteins, with frequent peaks showing the presence of flexible amino acids on the C-alpha backbone of the protein (**Fig. 13(b)**). MD simulation outcomes specify probable protein-ligand interactions in the form of histograms and heat maps (**Fig. 13(c), (d)**). The interface between protein and ligand comprises four types of bonds, hydrogen bonds (green), hydrophobic interaction (grey), ionic bonds (pink), and water bridges (blue). The amino acids residues Gln32, Ser134, Lys137, and His154 forms hydrogen bonds (green), Met145, Phe33, Leu131, Lys137, His154, Val157, Leu138, Ala161, and Leu158 from hydrophobic interaction (grey), and Glu28, Glu29, Gln32, Phe33, Lys127, Lys137, Asp151, Ser134, His154, Val157, and Arg164 forms water bridges (blue) respectively (**Fig. 13 (c)**). The ligand-protein contacts diagram is shown in (**Fig. 14(d)**).

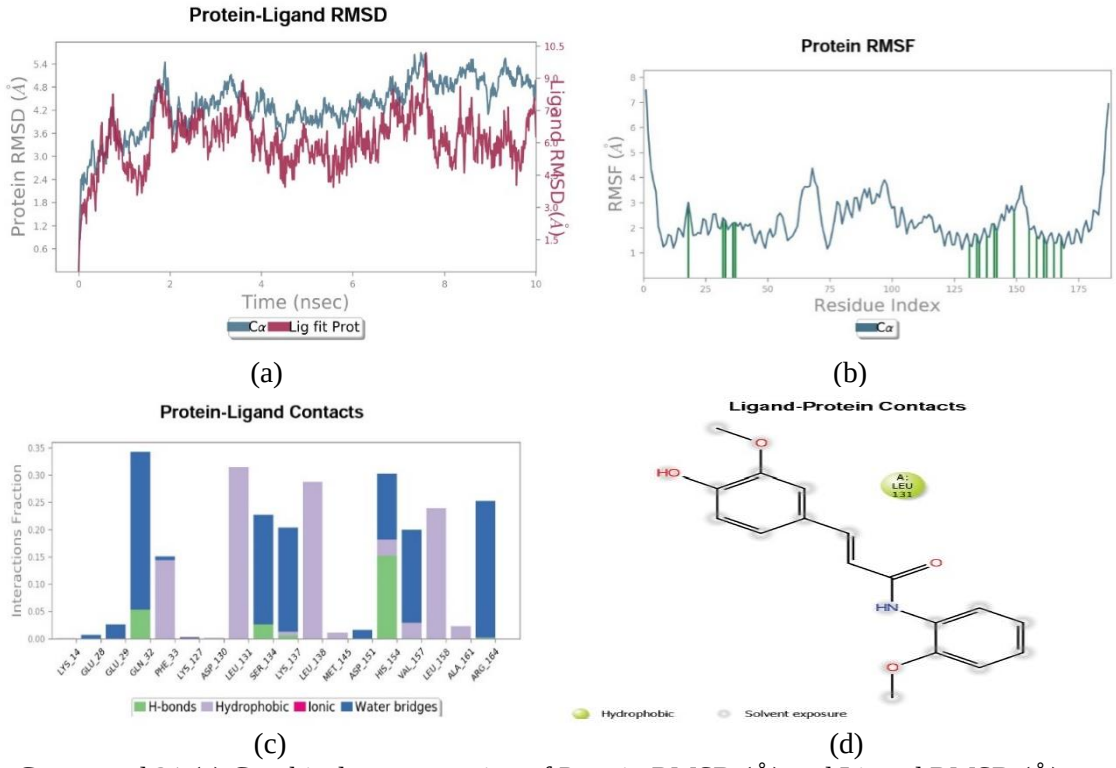

Fig. 14: Compound 21 (a) Graphical representation of Protein RMSD (Å) and Ligand RMSD (Å) versus time (ns), (b) Graphical representation of RMSF (Å) versus the residual index, (c) Histogram representation specifies probable protein-ligand interactions, (d) Ligand protein contact.

CONCLUSION

In this research work, various computational tools, i.e., 2D QSAR, molecular docking, molecular dynamics simulation and ADME studies of ferulic acid derivatives against ***E.Coli, S. Aureus,*** and ***B. Subtilis*** were performed. In 2D QSAR studies, molecular descriptors include topological parameters like valence third-order molecular connectivity index ($^3\chi^V$), valence first-order molecular connectivity index ($^1\chi^V$), Kier's third-order alpha shape index ($k\alpha^3$), and Balaban, lipophilic parameter like log P, electronic parameters like Vamp Lumo and total dipole, govern the antibacterial activity of ferulic acid derivatives. Molecular docking studies signify compounds **18, 15, 21, 32,** and **30** have the best docking score against protein transcriptional regulation (**PDB ID: 5X14**). Based on QSAR, molecular docking results, molecular dynamics simulation and binding interaction analysis, ADME studies were employed and showed an excellent ADME profile by the Lipinski rule of five. The study suggests that these compounds could be utilised as lead structures for advanced research in antimicrobial resistance.

Abbreviations

QSAR: Quantitative structure activity relationship; CADD: Computer Aided Drug Design; MIC: Minimum Inhibitory Concentration; MLR: Multiple Linear Regression; Log P: Partition Coefficient; pMIC: log of Minimum Inhibitory Concentration; µM: Micromol; ml: Milliliters; SA: ***S.Aureus;*** **EC:** ***E.Coli;*** **BS:** ***B.Subtilis;*** PDB: Protein data bank; MD: Molecular dynamics; LOO: Leave one out; DNA: Deoxyribonucleic acid; RNA: Ribonucleic acid; ADME; Adsorption Distribution Metabolism Excretion; HOMO: Highest occupied molecular orbital; LUMO: Lowest unoccupied molecular orbital; J: Balaban topological index; W: Wiener topological index; R: Randic topological index; µ: Total dipole; MR: Molecular Refractivity; RMSD: Root mean square deviation; RMSF: Root mean square fluctuation; SPC: Single point charge

Acknowledgements

The authors thank the Head of the Department of Pharmaceutical Sciences, Maharshi Dayanand University, Rohtak, for providing the necessary facilities to carry out this research work—special thanks to Vinod Devaraji and his team for guiding and learning Schrodinger software.

Authors' Contributions

Authors SY and BN designed the computational study; SY and MK carried out the 2D QSAR study; AS and DS carried out the molecular docking study; MA carried out the ADME study; SY and DB carried out the molecular dynamics simulation

of synthesised compounds; MK helped in critical revision of the manuscript. All authors read and approved the final manuscript.

Funding
Not applicable

Availability of data and materials
The datasets used and analysed during the current study are available from the corresponding author upon reasonable request.

Ethics approval and consent to participate
Not applicable

Conflict of interest
The authors declare no conflict of interest

Consent for publication
All authors of the research paper have approved the manuscript for submission.

Author details
[1,2]Faculty of Pharmaceutical Sciences, Deen Dayal Rustagi College of Pharmacy, Gurgaon, Haryana, India – 122504.[3,4,5]Faculty of Pharmaceutical Sciences, B.S. Anangpuria Institute of Pharmacy, Faridabad, Haryana, India – 121004.[6,7]Faculty of Pharmaceutical Sciences, Maharshi Dayanand University, Rohtak, Haryana, India – 124001.

REFERENCES

1. Emami S, Foroumadi A, Falahati M, Lotfali E, Rajabalian S, Ebrahimi SA, Farahyar S, Shafiee A. 2-Hydroxyphenacyl azoles and related azolium derivatives as antifungal agents. Bioorganic & medicinal chemistry letters. 2008 Jan 1;18(1):141-6.
2. Vila J, Pal T. Update on antibacterial resistance in low-income countries: factors favoring the emergence of resistance. The Open Infectious Diseases Journal. 2010 Sep 15;4(1).
3. Upreti N, Rayamajhee B, Sherchan SP, Choudhari MK, Banjara MR. Prevalence of methicillin resistant Staphylococcus aureus, multidrug resistant and extended spectrum β-lactamase producing gram negative bacilli causing wound infections at a tertiary care hospital of Nepal. Antimicrobial Resistance & Infection Control. 2018 Dec;7(1):1-0.
4. Elton L, Thomason MJ, Tembo J, Velavan TP, Pallerla SR, Arruda LB, Vairo F, Montaldo C, Ntoumi F, Abdel Hamid MM, Haider N. Antimicrobial resistance preparedness in sub-Saharan African countries. Antimicrobial Resistance & Infection Control. 2020 Dec;9:1-1.
5. Naylor NR, Atun R, Zhu N, Kulasabanathan K, Silva S, Chatterjee A, Knight GM, Robotham JV. Estimating the burden of antimicrobial resistance: a systematic literature review. Antimicrobial Resistance & Infection Control. 2018 Dec;7:1-7.
6. Hlasiwetz H, Barth L. Mittheilungen aus dem chemischen Laboratorium in Innsbruck I) Ueber einige Harze [Zersetzungsproducte derselben durch schmelzendes Kali]. Justus Liebigs Annalen der Chemie. 1866;138(1):61-76.
7. Clifford MN. Chlorogenic acids and other cinnamates–nature, occurrence, dietary burden, absorption and metabolism. Journal of the Science of Food and Agriculture. 2000 May 15;80(7):1033-43.
8. Anselmi C, Centini M, Andreassi M, Buonocore A, La Rosa C, Facino RM, Sega A, Tsuno F. Conformational analysis: a tool for the elucidation of the antioxidant properties of ferulic acid derivatives in membrane models. Journal of Pharmaceutical and Biomedical Analysis. 2004 Sep 3;35(5):1241-9.
9. Li W, Li N, Tang Y, Li B, Liu L, Zhang X, Fu H, Duan JA. Biological activity evaluation and structure–activity relationships analysis of ferulic acid and caffeic acid derivatives for anticancer. Bioorganic & Medicinal Chemistry Letters. 2012 Oct 1;22(19):6085-8.
10. Lee DG, Park Y, Kim MR, Jung HJ, Seu YB, Hahm KS, Woo ER. Anti-fungal effects of phenolic amides isolated from the root bark of Lycium chinense. Biotechnology letters. 2004 Jul;26:1125-30.
11. Murakami A, Nakamura Y, Koshimizu K, Takahashi D, Matsumoto K, Hagihara K, Taniguchi H, Nomura E, Hosoda A, Tsuno T, Maruta Y. FA15, a hydrophobic derivative of ferulic acid, suppresses inflammatory responses and skin tumor promotion: comparison with ferulic acid. Cancer Letters. 2002 Jun 28;180(2):121-9.
12. Stankova I, Chuchkov K, Shishkov S, Kostova K, Mukova L, Galabov AS. Synthesis, antioxidative and antiviral activity of hydroxycinnamic acid amides of thiazole containing amino acid. Amino acids. 2009 Jul;37:383-8.
13. Balasubashini MS, Rukkumani R, Viswanathan P, Menon VP. Ferulic acid alleviates lipid peroxidation in diabetic rats. Phytotherapy Research: An International Journal Devoted to Pharmacological and

Toxicological Evaluation of Natural Product Derivatives. 2004 Apr;18(4):310-4.
14. Folkman J. Angiogenesis in cancer, vascular, rheumatoid and other disease. Nature medicine. 1995 Jan 1;1(1):27-30.
15. Cheng YH, Yang SH, Yang KC, Chen MP, Lin FH. The effects of ferulic acid on nucleus pulposus cells under hydrogen peroxide-induced oxidative stress. Process Biochemistry. 2011 Aug 1;46(8):1670-7.
16. Abramson J, Giraud M, Benoist C, Mathis D. Aire's partners in the molecular control of immunological tolerance. Cell. 2010 Jan 8;140(1):123-35.
17. Adelman K, Lis JT. Promoter-proximal pausing of RNA polymerase II: emerging roles in metazoans. Nature Reviews Genetics. 2012 Oct;13(10):720-31.
18. Kapetanovic I. Computer-aided drug discovery and development (CADDD): in silico-chemico -biological approach. Chemico-biological interactions. 2008 Jan 30;171(2): 165-76.
19. Sliwoski G, Kothiwale S, Meiler J, Lowe EW. Computational methods in drug discovery. Pharmacological reviews. 2014 Jan 1;66(1): 334-95.
20. Chiu TL, So SS. Development of neural network QSPR models for Hansch substituent constants. 1. Method and validations. Journal of chemical information and computer sciences. 2004 Jan 26;44(1):147-53.
21. Oksel C, Winkler DA, Ma CY, Wilkins T, Wang XZ. Accurate and interpretable nanoSAR models from genetic programming-based decision tree construction approaches. Nanotoxicology. 2016 Aug 8;10(7):1001-12.
22. [22] Mahendran R, Jeyabaskar S, Francis AG. Computational Approaches for Identifying Drugs Against Alzheimer's Disease. Anchor Academic Publishing; 2017.
23. Borm PJ, Robbins D, Haubold S, Kuhlbusch T, Fissan H, Donaldson K, Schins R, Stone V, Kreyling W, Lademann J, Krutmann J. The potential risks of nanomaterials: a review carried out for ECETOC. Particle and fibre toxicology. 2006 Dec;3:1-35.
24. Hadavand Mirzaei H, Jassbi AR, Pirhadi S, Firuzi O. Study of the mechanism of action, molecular docking, and dynamics of anticancer terpenoids from Salvia lachnocalyx. Journal of Receptors and Signal Transduction. 2020 Jan 2;40(1):24-33.
25. Kumar S, Lim SM, Ramasamy K, Vasudevan M, Shah SA, Selvaraj M, Narasimhan B. Synthesis, molecular docking and biological evaluation of bis-pyrimidine Schiff base derivatives. Chemistry Central Journal. 2017 Dec;11(1):1-6.
26. Sharma D, Kumar S, Narasimhan B, Ramasamy K, Lim SM, Shah SA, Mani V. 4-(4-Bromophenyl)-thiazol-2-amine derivatives: synthesis, biological activity and molecular docking study with ADME profile. BMC chemistry. 2019 Dec;13(1):1-6.
27. Khatkar A, Nanda A, Kumar P, Narasimhan B. Synthesis and antimicrobial evaluation of ferulic acid derivatives. Research on Chemical Intermediates. 2015 Jan;41:299-309.
28. Hansch C, Fujita T. p-σ-π Analysis. A Method for the Correlation of Biological Activity and Chemical Structure. Journal of the American Chemical Society. 1964 Apr;86(8):1616-26.
29. Hansch C, Leo A, Unger SH, Kim KH, Nikaitani D, Lien EJ. Aromatic substituent constants for structure-activity correlations. Journal of medicinal chemistry. 1973 Nov;16(11):1207-16.
30. Hall LH, Kier LB. Issues in representation of molecular structure: the development of molecular connectivity. Journal of Molecular Graphics and Modelling. 2001 Dec 1;20(1):4-18.
31. Randic M. Characterization of molecular branching. Journal of the American Chemical Society. 1975 Nov;97(23):6609-15.
32. Randić M. Comparative regression analysis. Regressions based on a single descriptor. Croatica Chemica Acta. 1993 Jul 1;66(2):289-312.
33. Wiener H. Relation of the physical properties of the isomeric alkanes to molecular structure. Surface tension, specific dispersion, and critical solution temperature in aniline. The Journal of Physical Chemistry. 1948 Jun;52(6):1082-9.
34. Madhavi Sastry G, Adzhigirey M, Day T, Annabhimoju R, Sherman W. Protein and ligand preparation: parameters, protocols, and influence on virtual screening enrichments. Journal of computer-aided molecular design. 2013 Mar;27:221-34.
35. Kumar S, Singh J, Narasimhan B, Shah SA, Lim SM, Ramasamy K, Mani V. Reverse pharmacophore mapping and molecular docking studies for discovery of GTPase HRas as promising drug target for bis-pyrimidine derivatives. Chemistry Central Journal. 2018 Dec;12:1-1.
36. Van Den Driessche G, Fourches D. Adverse drug reactions triggered by the common HLA-B* 57: 01 variant: a molecular docking study.

Journal of cheminformatics. 2017 Dec;9(1):1-7.
37. Sharma V, Sharma PC, Kumar V. In silico molecular docking analysis of natural pyridoacridines as anticancer agents. Advances in Chemistry. 2016 Nov;2016(5409387):1-9.
38. Friesner RA, Murphy RB, Repasky MP, Frye LL, Greenwood JR, Halgren TA, Sanschagrin PC, Mainz DT. Extra precision glide: Docking and scoring incorporating a model of hydrophobic enclosure for protein− ligand complexes. Journal of medicinal chemistry. 2006 Oct 19;49(21):6177-96.
39. Lenselink EB, Louvel J, Forti AF, van Veldhoven JP, de Vries H, Mulder-Krieger T, McRobb FM, Negri A, Goose J, Abel R, van Vlijmen HW. Predicting binding affinities for GPCR ligands using free-energy perturbation. ACS omega. 2016 Aug 31;1(2):293-304.
40. Meraj K, Mahto MK, Christina NB, Desai N, Shahbazi S, Bhaskar M. Molecular modeling, docking and ADMET studies towards development of novel Disopyramide analogs for potential inhibition of human voltage gated sodium channel proteins. Bioinformation. 2012;8(23):1139.
41. Bowers KJ, Chow E, Xu H, Dror RO, Eastwood MP, Gregersen BA, Klepeis JL, Kolossvary I, Moraes MA, Sacerdoti FD, Salmon JK. Scalable algorithms for molecular dynamics simulations on commodity clusters. InProceedings of the 2006 ACM/IEEE Conference on Supercomputing 2006 Nov 11 (pp. 84-es).
42. Jorgensen WL, Maxwell DS, Tirado-Rives J. Development and testing of the OPLS all-atom force field on conformational energetics and properties of organic liquids. Journal of the American Chemical Society. 1996 Nov 13;118(45):11225-36.
43. Shivakumar D, Williams J, Wu Y, Damm W, Shelley J, Sherman W. Prediction of absolute solvation free energies using molecular dynamics free energy perturbation and the OPLS force field. Journal of chemical theory and computation. 2010 May 11;6(5):1509-19.
44. Martyna GJ, Klein ML, Tuckerman M. Nosé–Hoover chains: The canonical ensemble via continuous dynamics. The Journal of chemical physics. 1992 Aug 15;97(4):2635-43.
45. Toukmaji AY, Board Jr JA. Ewald summation techniques in perspective: a survey. Computer physics communications. 1996 Jun 1;95(2-3):73-92.
46. Narasimhan B, Kumari M, Jain N, Dhake A, Sundaravelan C. Correlation of antibacterial activity of some N-[5-(2-furanyl)-2-methyl-4-oxo-4H-thieno [2, 3-d] pyrimidin-3-yl]-carboxamide and 3-substituted-5-(2-furanyl)-2-methyl-3H-thieno [2, 3-d] pyrimidin-4-ones with topological indices using Hansch analysis. Bioorganic & medicinal chemistry letters. 2006 Sep 15;16(18):4951-8.